Journal of Peptide Science
J. Peptide Sci. **10**: 138–148 (2004)
Published online 10 November 2003 in Wiley InterScience (www.interscience.wiley.com). DOI: 10.1002/psc.505

JOURNAL OF PEPTIDE SCIENCE

Complete Structure Determination of the A Chain of Mistletoe Lectin III from *Viscum album* L. ssp. *album*

ROLAND WACKER,[a] STANKA STOEVA,[a] KAROLA PFÜLLER,[b] UWE PFÜLLER[b] and WOLFGANG VOELTER[a]*

[a] Abteilung für Physikalische Biochemie der Universität Tübingen, Hoppe-Seyler-Str. 4, D-72076 Tübingen, Germany
[b] Institut für Phytochemie, Universität Witten/Herdecke GmbH, Stockumer-Str. 10, D-58448 Witten-Annen, Germany

Received 30 April 2003
Accepted 13 May 2003

Abstract: The complete primary structure of the A chain of mistletoe lectin III (ML3A), a type II ribosome-inactivating protein, was determined using proteolytic digests of ML3A, HPLC separation of the peptides, Edman degration and MALDI-MS. Based on our results, ML3A consists of 254 amino acid residues, showing a high homology to the A chain of isolectin ML1 with only 24 amino acid residue exchanges. A striking important structural difference compared with ML1A is the lack of the single N-glycosylation site in ML3A due to an amino acid exchange at position 112 (ML1A: $N^{112}GS \Rightarrow$ ML3A: $T^{112}GS$). The alignment of ML3A with the A chains of ML1, isoabrins, ricin D, *Ricinus communis* agglutinin and three lectins, identified from the Korean mistletoe *Viscum album* ssp. *coloratum*, demonstrates the rigid conservation of all amino acid residues, responsible for the RNA-N-glycosidase activity as reported for ricin D. In addition, the fully determined primary structure of ML3A will give further information about the biological mechanism of mistletoe lectin therapy.

Keywords: mistletoe; lectins; isolectins; ribosome-inactivating protein

INTRODUCTION

Since ancient times, extracts of the semiparasitic European plant mistletoe, *Viscum album L. ssp. album*, have been used for therapeutic purposes. While in the past the medical use of mistletoe originated from mythological and anthroposophical considerations, recently, specific biological effects were identified for different mistletoe ingredients [1,2]. From mistletoe extracts several glycoproteins were isolated, the mistletoe lectins, showing effects on cells of the immune system and apoptotic properties [3,4]. Mistletoe lectin I (ML1) is a toxic, ribosome-inactivating protein of type II (RIP-II), consisting of two protein chains linked by an intermolecular disulphide bridge [5]. Other prominent representatives of this plant protein family are ricin, *Ricinus communis* agglutinin or abrin. Common to all RIPs of type II is their RNA-N-glycosidase activity, located in their A chains, causing depurination of a single adenine residue of eukaryotic ribosomes [6] and thereby preventing protein biosynthesis. In the ML1B chain (32 kDa) specific carbohydrate-binding lectin motifs were identified, responsible for binding to the target cell and the transport of the A chain into the cytosol [7].

It has been shown that subcutaneous injections of nontoxic doses of ML1 cause immunomodulatory effects, such as the proliferation of natural killer cells and lymphocyte subpopulations, the enhancement of the phagocytic activity of

Abbreviations: ML, mistletoe lectin; RCA, *Ricinus communis* agglutinin; RIP, ribosome-inactivating protein.

*Correspondence to: Professor Wolfgang Voelter, Abteilung für Physikalische Biochemie der Universität Tübingen, Hoppe-Seyler-Str. 4, D-72076 Tübingen, Germany.

granulocytes and monocytes and the release of inflammatory cytokines [8–12]. In addition, an improvement in the life quality of cancer patients undergoing mistletoe therapy was observed, most probably due to an increase of β-endorphin release [13,14].

For most RIPs of type II, isolectins with modified biophysical and biological properties were identified [15–20], and, for mistletoe lectin, at least three isoforms, ML1–ML3, were isolated [21]. These isoforms have different monosaccharide specificities and molecular masses as estimated by SDS-PAGE. ML1 specifically binds to D-galactose, ML3 to N-acetyl-D-galactosamine and for ML2 binding sites for both carbohydrates with similar binding constants were detected [21–23]. Recently, the complete primary structure of ML1A was reported based on Edman degration sequencing [24,25]. The crystal structure of ML1 could be established by x-ray crystallographic studies based on these sequencing data [5]. Though much effort has been made to elucidate the structure–activity relationships for the different mistletoe lectins, clear-cut answers are still unavailable. Despite their structural similarity, there are indications for a heterogeneous cytotoxicity against cell lines [7,26], an ability to release cytokines [27,28] or induction of apoptosis [29,30].

To understand the structure–function relationship of the different mistletoe lectins on a molecular basis, a detailed knowledge of their molecular structures is essential. Therefore the purification and complete primary structure of the ML3A chain from *Viscum album* ssp. *album* was undertaken and is reported in this communication.

MATERIALS AND METHODS

Materials

The sequencing reagents were obtained from the instrument supplier PE Biosystems (Weiterstadt, Germany). The chemicals used for MALDI-MS were purchased from Sigma (Taufkirchen, Germany). Proteases were obtained in sequencing grade quality from Boehringer Mannheim (Mannheim, Germany). All other chemicals were obtained from Merck (Darmstadt, Germany). The ML3A chain was kindly provided by Professor U. Pfüller (Institut für Phytochemie, Universität Witten/Herdecke) and isolated according to references [22,24].

Enzymatic Digestion

The digestion of ML3A (2.0 mg) with endoproteinase AspN was performed in 2 ml of 50 mM sodium

Table 1 Results of the Sequence Analysis of Peptides, Isolated from the Endo-proteinase AspN digest of ML3A. Peptides are Labelled According to Figure 1

Peptide	Position	Sequence	M_{th}[a] (Da)	M_{ob}[b] (Da)
D1a	1–5	YERLR	735.8	737.2
D1b	6–14	LRVTHQTTG	1012.1	1012.6
D2	15–25	DEYFRFITLLR	1472.7	n.d.
D3a	26–42	DYVSSGSFSNEIPLLRQ	1912.1	1913.6
D3b	43–48	STIPVS	602.7	(Na) 627.3
D4	49–63	DAQRFVLVELTNQGG	1646.8	1647.8
D5	64–70	DSITAAI	689.8	690.7
D6	71–83	DVTNLYVVAYQAG	1412.5	(Na) 1435.5
D7	84–90	DQSYFLR	928.0	929.7
D8a	91–101	DAPNGAERHLF	1226.3	1228.7
D8b	102–116	TGTARSSLPFTGSYT	1545.7	1547.1
D9	117–125	DLERYAGHR	1116.2	1117.2
D10	126–???	DQIPLGIEELIQSVSALRYPGGSTRAQARSILILIQMISEA. . .	n.d.	n.d.
D11	179–188	DINSGESFLP	1078.1	1078.9
D12	189–210	DMYMLELETSWGQQSTQVQQST	2590.8	(Na) 2613.5
D13	211–???	DGVFNNPFRLAISTGNFVTLSNVRDVIASLAIMLFV. . .	n.d.	n.d.

[a] Calculated peptide mass.
[b] Observed peptide mass ($M + H^+$); (Na): ($M + Na^+$); n.d.: not determined.

Table 2 Results of the Sequence Analysis of Peptides, Isolated from the Chymotryptic Digest of ML3A. Peptides are Labelled According to Figure 1

Peptide	Position	Sequence	M_{th}[a] (Da)	M_{ob}[b] (Da)
C1	1–4	YERL	579.6	580.9
C2	7–17	RVTHQTTGDEY	1306.3	1306.5
C3	25–33	RDYVSSGSF	1017.1	1018.3
C4	34–39	SNEIPL	671.7	(Na) 696.4
C5	40–53	LRQSTIPVSDAQRF	1617.9	1619.9
C6	69–75	AIDVTNLY	908.0	908.0
C7	77–80	VVAY	450.5	450.9
C8	81–87	QAGDQSY	767.8	771.0
C9	88–101	FLRDAPNGAERHLF	1642.8	1643.6
C9A	89–101	LRDAPNGAERHLF	1495.7	1499.0
C9B	89–101	LRDAPRGAETHLF	1482.7	1484.5
C10A	102–111	TGTARSSLPF	1036.1	1036.7
C10B	102–111	TGTTRSSLPF	1066.2	1068.1
C11	112–121	TGSYTDLERY	1204.2	1206.0
C12	122–130	AGHRDQIPL	1006.1	1008.5
C13	131–142	GIEELIQSVSAL	1258.4	(Na) 1282.6
C14	143–150	RYPGGSTR	893.0	894.8
C15	160–169	IQMISEAARF	1165.4	1167.8
C16	170–174	NPIFW	675.8	676.3
C17	175–191	RVRQDINSGESFLPDMY	2027.2	2028.8
C18	192–199	MLELETSW	1008.1	(Na) 1032.5
C19	200–214	GQQSTQVQQSTDGVF	1609.7	1611.4
C20	215–218	NNPF	490.5	492.0
C21	219–230	RLAISTGNFVTL	1291.5	1292.3
C22	231–240	SNVRDVIASL	1073.2	1074.6
C23	241–245	AIMLF	593.8	593.6
C24	246–254	VCGERPSSS	921.0	922.3

[a] Calculated peptide mass (M).
[b] Observed peptide mass ($M + H^+$); (Na): ($M + Na^+$).

Table 3 Results of Selected Peptides, Obtained from a Tryptic Digest of ML3. Peptides are Labelled According to Figure 1

Peptide	Position	Sequence	Mth[a] (Da)	Mob[b] (Da)
T17A	99–106	HLFTGTAR	902.0	903.4
T17B	99–106	HLFTGTTR	932.0	933.2
T40	169–175	FNPIFWR	979.1	979.7

[a] Calculated peptide mass (M).
[b] Observed peptide mass ($M + H^+$).

phosphate, 2 M urea, pH 7.8, at 37°C with 3 µg protease for 4 h. The chymotryptic digestion of ML3A (5.0 mg) was carried out using 2 ml 0.1 M Tris/HCl, 10 mM $CaCl_2$, pH 7.8, in the presence of 100 µg chymotrypsin at 37°C with stirring. After 15 min, another portion of 50 µg enzyme was added and the mixture was incubated for another 15 min. A third control series of digested peptides was obtained by treating 5.0 mg of ML3 with 250 µg trypsin in five portions for 18 h at 37°C in 0.2 M Tris/HCl, 10% (v/v) CH_3CN, pH 8.5.

Fractionation of the Peptides

The enzymatic digest was acidified with TFA until a pH of 3 was obtained and centrifuged from unsoluble material. The soluble peptide digest were fractionated via RP-HPLC on a Gromsil C-18 column (100-5 ODS, 4.6 × 250 mm) with a linear gradient of acetonitrile, containing 0.1% (v/v) TFA at a flow rate of 1 ml/min. The eluted peptides were detected by UV absorbance at 220 nm, collected manually and recovered by lyophilization.

Table 4 Similarity Matrix of Identical (above) and Similar (below) Amino Acid Residues between Related Sequences in Percentage (above the diagonal) and in Numbers of Amino Acid Residues (below the diagonal), respectively. The diagonal itself shows the number of amino acid residues for the individual proteins. ABRA: abrin A [16], ABRB: abrin B [16], ABRC: abrin C [16], RCA: *Ricinus communis* agglutinin [15], RICD: ricin D [45], ML1Ap: mistletoe lectin 1 [24], ML1Ad: mistletoe lectin 1 [44], ML1A': mistletoe lectin 1' [24], ML3A: mistletoe lectin 3, kML1A-kML3A: Korean mistletoe lectins 1–3 [36]

	ABRB	ABRC	ABRA	kML1A	KML2A	ML3A	ML1A'	ML1Ap	ML1Ad	KML3A	RCA	RICD
ABRB	250	83%	80%	39%	41%	40%	39%	39%	38%	38%	38%	40%
		91%	89%	59%	58%	58%	58%	58%	57%	56%	53%	55%
ABRC	209	**251**	81%	42%	43%	42%	42%	41%	40%	40%	36%	39%
	230		92%	58%	58%	58%	59%	59%	58%	55%	52%	54%
ABRA	201	205	**251**	42%	42%	42%	42%	41%	40%	39%	36%	38%
	225	232		58%	58%	58%	58%	58%	57%	56%	50%	52%
KML1A	102	108	108	**254**	92%	90%	90%	87%	89%	84%	35%	37%
	152	150	151		97%	95%	93%	92%	93%	89%	53%	54%
KML2A	105	111	110	235	**254**	85%	86%	86%	88%	80%	36%	38%
	150	151	149	247		93%	93%	94%	94%	87%	53%	54%
ML3A	104	108	108	231	217	**254**	96%	90%	91%	84%	35%	36%
	150	150	151	242	237		97%	94%	94%	89%	52%	54%
ML1A'	102	108	108	230	219	245	**254**	93%	92%	83%	36%	37%
	149	152	149	238	237	247		96%	94%	87%	53%	54%
ML1Ap	100	105	105	223	220	230	237	**254**	97%	82%	36%	38%
	150	153	150	236	239	240	245		98%	87%	54%	55%
ML1Ad	99	104	104	227	224	233	235	248	**254**	83%	35%	36%
	147	149	147	238	241	241	241	250		88%	52%	54%
KML3A	100	104	103	217	206	218	215	211	215	**256**	35%	37%
	146	144	145	230	225	229	225	226	228		52%	53%
RCA	102	99	97	96	99	95	97	99	95	95	**266**	93%
	143	142	136	144	143	142	143	145	142	142		96%
RICD	108	106	102	101	103	99	101	102	99	100	250	**267**
	148	147	142	147	146	145	146	149	145	144	258	

Insoluble peptides, precipitated during the acidification step after proteolysis, were separated by centrifugation, reconstituted with 300 µl of concentrated formic acid, immediately diluted to 1 ml with distilled water and filtered through a microconcentrator (Millipore, Eschborn, Germany; poresize: 0.22 µm). The soluble peptides in the filtrate were separated by RP-HPLC on a Parcosil ProRP 300 C4 column (Serva, Heidelberg, Germany; dimensions: 4.6 × 100 mm) with a linear gradient of acetonitrile, containing 0.1% (v/v) TFA at 1 ml/min flow rate.

Sequence Analysis

Automated Edman degradation was performed using an Applied Biosystems pulsed liquid sequencer model 473A (Applied Biosystems, Weiterstadt, Germany) with online analysis of the phenylthiohydantoin (PTH) derivatives. The sequence of the peptides, dissolved in 0.1% (v/v) TFA and spotted onto polybrene-coated filters, was evaluated by comparing the HPLC chromatograms of standard PTH-derivatized amino acids with the profiles produced by sequential Edman degradation of the protein fragments.

Mass Spectrometric Analysis

Matrix-assisted laser desorption ionization (MALDI) mass spectra were obtained from the isolated peptides using a Kratos Kompact MALDI II instrument (Shimadzu, Torrance (Ca), USA). The samples were dissolved in 0.1% (v/v) TFA in water, aliquots of 0.5 µl were mixed with 0.5 µl matrix solution and applied on a stainless steel slide. The droplet was allowed to dry at atmospheric pressure and the sample slide was loaded for analysis into the mass spectrometer. As the matrix,

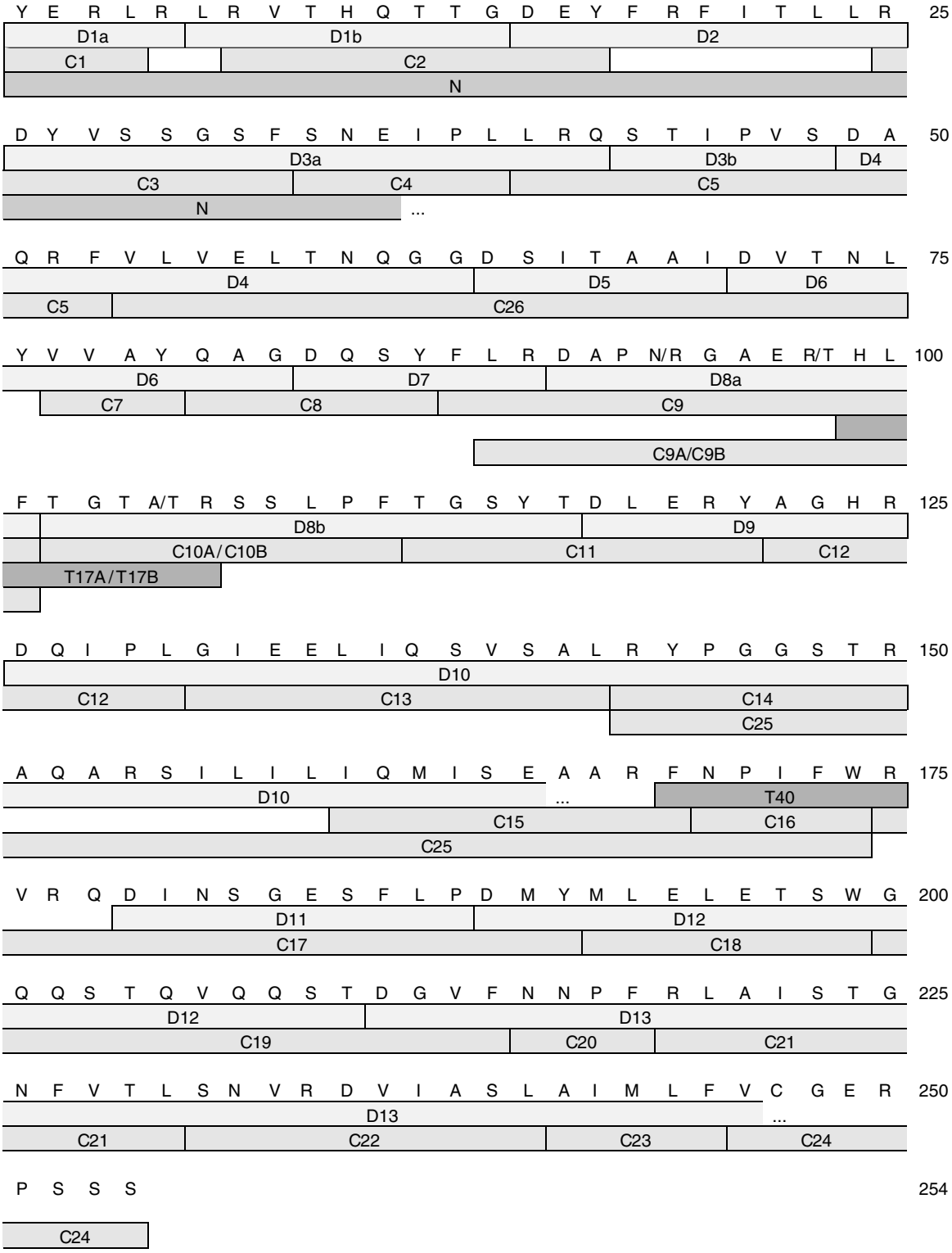

Figure 1 Amino acid sequence and sequencing strategy of the A chain of mistletoe lectin III. D and C indicate peptides from endoproteinase AspN and chymotrypsin digests, respectively. N represents the aminoterminal sequence without digestion, while T indicates ML3A peptides from a tryptic cleavage of ML3 holoprotein.

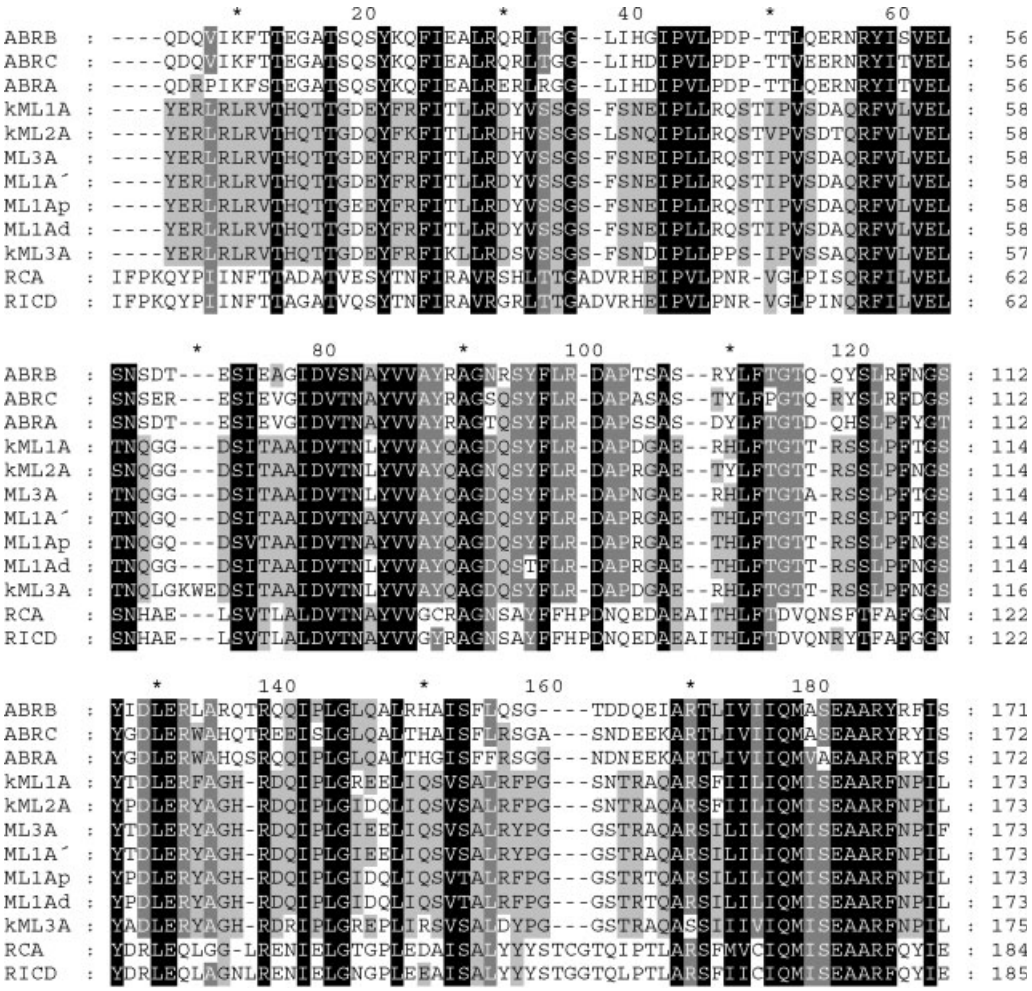

Figure 2 Multiple sequence alignment of the A chain of ML3 and the A chain sequences of abrin A (ABRA) [16], abrin B (ABRB) [16], abrin C (ABRC) [16], *Ricinus communis* agglutinin (RCA) [15], ricin D (RICD) [45], mistletoe lectin I (ML1Ap, ML1Ad, determined by protein [24] and nucleic acid sequencing [44], respectively), ML1A isoform ML1A' [24] and the translated nucleic acid sequences of the three lectins isolated from the Korean mistletoe *Viscum album* ssp. *coloratum* [36]. Similar amino acid residues are shaded using a Blosum 62 [46] scoring table.

a mixture of α-cyano-4-hydroxycinnamic acid and 2,5-dihydroxybenzoic acid in 70% acetonitrile and 0.1% TFA was used. MALDI-MS spectra were calibrated using several peptide ion peaks (e.g. substance P, m/z 1348.7; bovine ubiquitin, m/z 8565.9) as standards.

Sequence Alignment

The determined sequences were compared with published protein sequences using the PSI-BLAST program [31]. Multiple sequence alignment was performed and presented applying the software ClustalX [32] and GeneDoc [33].

RESULTS

The mistletoe lectin III A chain was isolated according to reference [22]. A first *N*-terminal sequencing trial of native ML3A resulted in 26 unambiguously identified degration steps. Two different enzymatic digests were performed with endoproteinase AspN and chymotrypsin, respectively, and fractionated by RP-HPLC. Each separated fraction of cleavaged peptides was identified by automated amino acid sequence analysis and MALDI-MS (Tables 1, 2 and Figure 1). A third, tryptic digest of ML3, enabled the determination of three more peptides (Table 3). The masses of the peptide fragments, calculated on basis of the sequence data, could be confirmed by

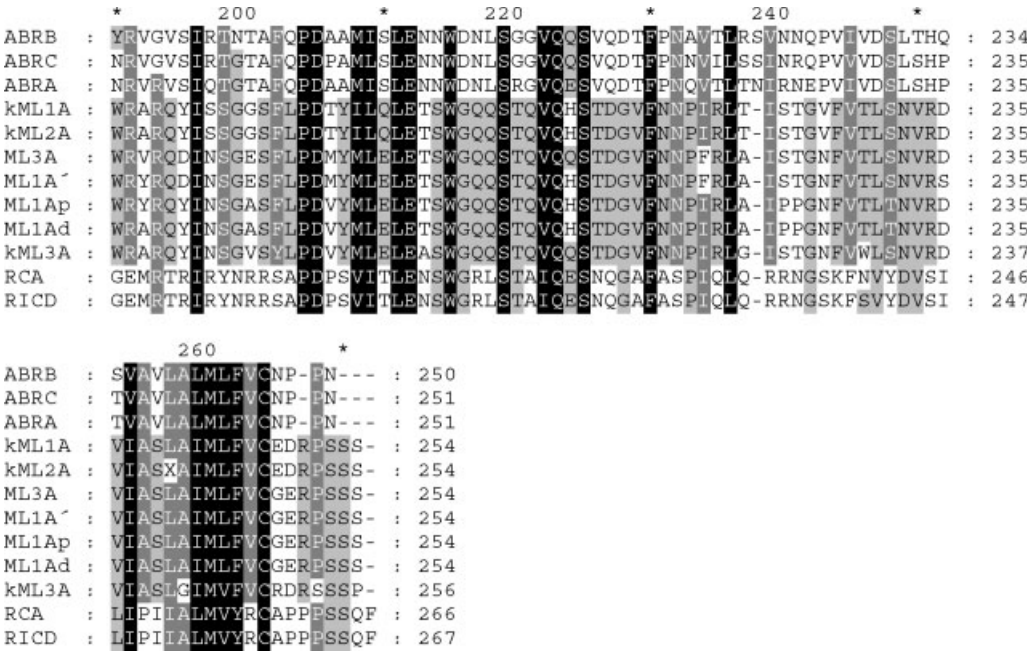

Figure 2 (*Continued*).

MALDI-MS. From these sets of overlapping peptide fragments the complete primary structure of the A chain was established. ML3A is composed of 254 amino acid residues and has a calculated molecular mass of 28427 Da which is in accordance with published SDS-gel electrophoretic results [21–23] and thus lower compared with that of ML1A (28480 Da without glycosylation). None of the peptide fragments, collected from different enzymatic digests of ML3A showed a positive orcinol colour reaction which is in accordance with the sequencing data, revealing no N-glycosylation site. The ML3A chain is therefore a non-glycosylated protein in contrast to ML1A [34,35].

The amino acid residue allocated to position 247 in ML3A could not be detected via Edman degradation, indicating a cysteine residue. Based on homology considerations [5,24] and confirmed by mass spectrometry (Table 2), a cysteine residue was, indeed, assigned to this position.

Peptides with substitutions at positions 94, 98 and 105 were observed in fractions of the two digests simultaneously and the existence of a ML3A isoform is suggested (Table 3), although these peptides could result from ML1A contaminations too.

DISCUSSION

The primary structure of ML3A shares a very high homology to ML1A and other RIPs of type II (Figures 2 and 3). Comparing the sequence of ML1A with that of ML3A, 91% or 230 of the 254 amino acid residues are identical and 10 amino acid exchanges are conservative substitutions resulting in 95% similarity. The identity and similarity values of the primary structure of ML3A compared with the related three mistletoe lectins from *Viscum album* ssp. *coloratum*, kML1A, kML2A and kML3A [36], vary from 85% to 90% and 89% to 93%, respectively. The phylogenetic distance of ML3A from *Viscum album* ssp. *album* to the A-chains of lectins from *Abrus precatorius* and *Ricinus communis* is reflected by a percentage of 58% to 65% overall sequence substitutions and still 42% to 48% nonconservative substitutions. Beside these amino acid exchanges, alignment of different lectins demonstrates a rigid conservation of all residues that might be responsible for the RNA-N-glycosidase activity, as proposed for ricin D [37–39]: all listed A chain sequences share the invariant residues Y^{80}, V^{81}, G^{121}, Y^{123}, E^{177} and R^{180}. From these findings it is most likely that all these RIPs act on RNA via a similar mechanism and with a highly conserved active site.

Moreover, the above mentioned isoform ML1A' shows the highest sequence identity compared with the ML3A primary structure of all sequences, listed in Figure 2 (96% identity and 97% sequence similarity) and shares all characteristic exchanges, found in ML3A. Furthermore, it was reported that

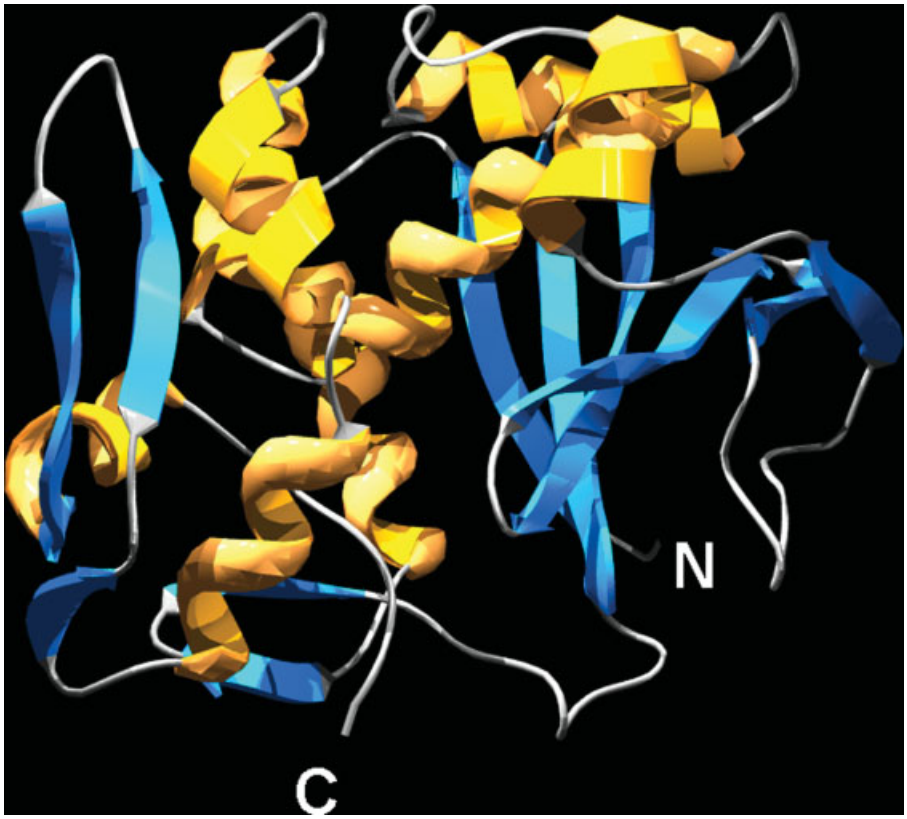

Figure 3 Cartoon plot of the ML3 A chain homology model. N and C marks the *N*- and the *C*-terminus of the protein, respectively. α-Helices are drawn in yellow and β-sheet structures in blue. The homology model of ML3A was prepared by the SWISS-Model server in the first approach mode using x-ray diffraction-derived templates from the pdb database 1CE7 (ML1), 1ABR (abrin a), 1RTC (ricin). Figures 3 and 4 were drawn using the programs Swiss-PdbViewer 3.51 [41–43] and Pov-Ray 3.1 [47].

ML1 is a mixture of three dimeric isoforms, differing by molecular weight and glycosylations of the A-chain: $(A^1B)_2$, $(A^2B)_2$ and (A^1BBA^2) [22]. We suggest that the described, unglycosylated A^2 chain of lower molecular weight is identical to ML1A' or at least very similar, if not identical to the structure of ML3A. It is worthwhile mentioning that the Korean mistletoe lectin kML1A lacks any glycosylation site in its A chain like the European ML3A chain, whereas for the two other Korean lectins kML2 and kML3, NGS-glycosylated A chains were determined, also found for ML1 [36].

Based on the results of the sequence analysis, a homology model of ML3A was created using the automated algorithm by the SWISS-Model server in the first approach mode [40–42] and the following x-ray diffraction-derived templates from the pdb database [43]: 1CE7 (ML1), 1ABR (abrin a), 1RTC (ricin). The coordinates calculated by the automated modelling program are visualized in a ribbon cartoon plot (Figure 3). The model indicates a globular structure of ML3A with distinct ratios of α-helix and β-sheet structure elements.

As expected, the peptide backbone trace overlay of the ML3A model and the x-ray structure of ML1A (Figure 4) demonstrates a strong conservation of the secondary structure elements and the overall protein fold. Also, the amino acid residues (Y^{80}, V^{81}, G^{121}, Y^{123}, E^{177} and R^{180}) of the RNA cleavage sites are in both structures identical and closely arranged in space. One main difference is the glycosylation of the ML1A chain at Asn^{122} in the immediate neighbourhood of the catalytic active centre. Despite the close similarity of ML3A and ML1A, remarkable differences between ML1 and ML3 concerning their biological activities were reported, e.g. tenfold higher cytotoxicity of ML3 against Molt 4 cells compared with ML1 [26]. A recombinant non-glycosylated ML1A-chain showed only one fifth of the toxicity compared with the native glycosylated ML1A chain

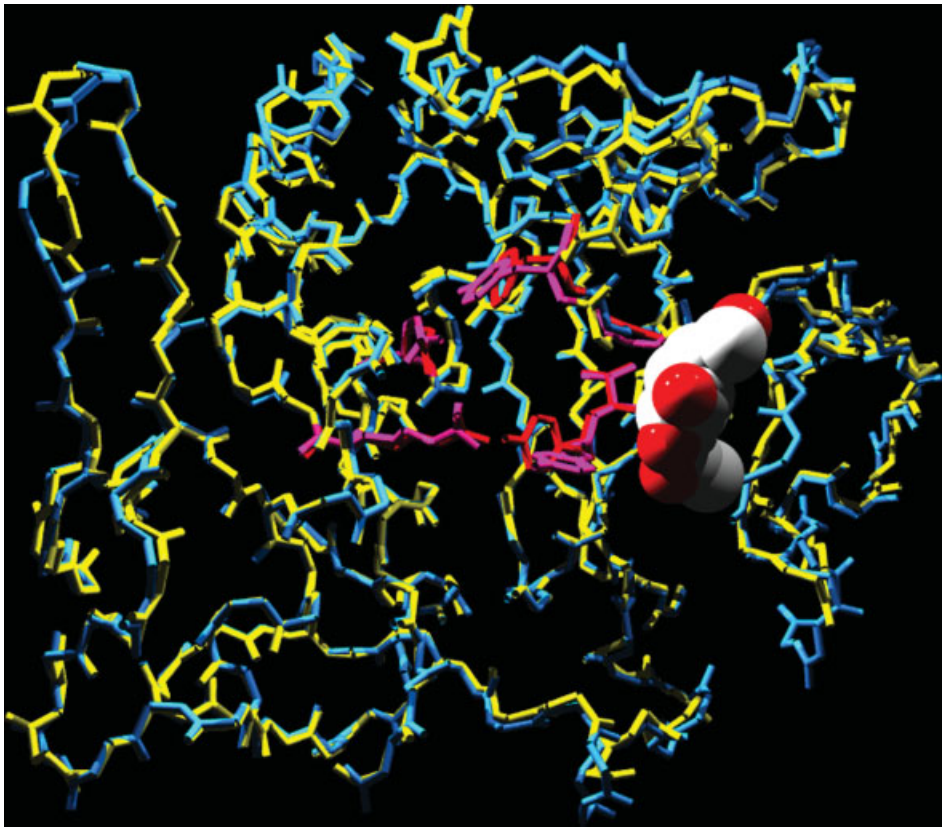

Figure 4 Peptide backbone overlay of the A chains of ML3 (blue, model) and ML1 (yellow, PDB access code 2AAI). The amino acid residues of the enzymatic active centre are shaded in red (ML1) and pink (ML3), respectively. The first N-acetylglucosamine residue of the N-type glycan connected to residue Asn^{A107} of mistletoe lectin I is represented as white and red balls.

in the RIP activity assay [44]. We suggest that the different biological activities found for mistletoe lectins with glycosylated and non-glycosylated A chains are at least in part caused by the presence or absence, respectively, of the carbohydrate chain close to the RNA-binding sites.

REFERENCES

1. Voelter W, Huguet Soler M, Stoeva S, Betzel C, Eschenburg S, Krauspenhaar R. First three-dimensional model building study of the A chain of mistletoe lectin I. *GIT Lab. J. Int. Ed.* 1997; **1**: 32–34.
2. Voelter W, Wacker R, Franz M, Maier T, Stoeva S. Complete structural characterization of a chitin-binding lectin from mistletoe extracts. *J. Prakt. Chem.* 2000; **342**: 812–818.
3. Bantel H, Engels IH, Voelter W, Schulze-Osthoff, Wesselborg S. Mistletoe lectin activates Caspase-8/FLICE independently of death receptor signaling and enhances anticancer drug-induced apoptosis. *Cancer Res.* 1999; **59**: 2083–2090.
4. Langer M, Möckel B, Eck J, Zinke H, Lentzen H. Site-specific mutagenesis of mistletoe lectin: the role of RIP activity in apoptosis. *Biochem. Biophys. Res. Commun.* 1999; **264**: 944–948.
5. Krauspenhaar R, Eschenburg S, Perbandt M, Kornilov V, Konareva N, Mikailova I, Stoeva S, Wacker R, Maier T, Singh T, Mikhailov M, Voelter W, Betzel C. Crystal structure of mistletoe lectin I from *Viscum album*. *Biochem. Biophys. Res. Commun.* 1999; **257**: 418–424.
6. Endo Y, Kunio T, Franz H. The site of action of the A-chain of mistletoe lectin I on eukaryotic ribosomes: The RNA N-glycosidase activity of the protein. *FEBS Letters* 1988; **231**: 378–380.
7. Doser C, Doser M, Hülsen H, Mechelke F. Influence of carbohydrates on the cytotoxicity of an aqueous mistletoe drug and of purified mistletoe lectins tested on human T-leukemia cells. *Arzneimittelforsch./Drug Res.* 1989,; **39**: 647–651.
8. Hajto T, Hostanska K, Gabius HJ. Modulatory potency of the beta-galactoside-specific lectin from mistletoe

extract (Iscador) on the host defense system *in vivo* in rabbits and patients. *Cancer Res.* 1989; **49**: 4803–4808.
9. Hajto T, Hostanska K, Frei K, Rordorf C, Gabius HJ. Increased secretion of tumor necrosis factors alpha, interleukin 1, and interleukin 6 by human mononuclear cells exposed to beta-galactoside-specific lectin from clinically applied mistletoe extract. *Cancer Res.* 1990; **50**: 3322–3326.
10. Beuth J, Stoffel B, Ko HL, Jeljaszewicz J, Pulverer G. Immunomodulating ability of galactoside-specific lectin standardized and depleted mistletoe extract. *Arzneimittelforsch./Drug Res.* 1995; **45**: 1240–1242.
11. Hajto T, Hostanska K, Fischer S, Saller R. Immunomodulatory effects of *Viscum album* agglutinin-I on natural immunity. *Anticancer Drugs* 1997; **8**: 43–46.
12. Baxevanis CN, Voutsas IF, Soler MH, Gritzapis AD, Tsitsilonis OE, Stoeva S, Voelter W, Arsenis P, Papamichail M. Mistletoe lectin I-induced effects on human cytotoxic lymphocytes. I. Synergism with IL-2 in the induction of enhanced LAK cytotoxicity. *Immunopharmacol. Immunotoxicol.* 1998; **20**: 355–372.
13. Heiny BM, Beuth J. Das Lektin der Mistel als Immunmodulator: Effektorwirkung auf β-Endorphin- und Zytokonfreisetzung bei Mammakarzinompatientinnen. *Dtsch. Zschr. Onkol.* 1994; **26**: 103–108.
14. Heiny BM, Beuth J. Mistletoe extract standardized for the galactoside-specific lectin (ML-1) induces beta-endorphin release and immunopotentiation in breast cancer patients. *Anticancer Res.* 1994; **14**: 1339–1342.
15. Roberts LM, Lamb FI, Pappin DJC, Lord JM. The primary sequence of *Ricinus communis* agglutinin. Comparison with ricin. *J. Biol. Chem.* 1985; **260**: 15 682–15 686.
16. Hung CH, Lee MC, Lee TC, Lin JY. Primary structure of three distinct isoabrins determined by cDNA sequencing. *J. Mol. Biol.* 1993; **229**: 263–267.
17. Ling J, Liu W, Wang TP. Simultaneous existence of two types of ribosome-inactivating proteins in the seeds of *Cinnamonum camphera* — characterization of the enzymatic activities of these cytotoxic proteins. *Biochim. Biophys. Acta* 1995; **1252**: 15–22.
18. Van Damme EJM, Hao Q, Charels D, Barre A, Rouge P, Van Leuven F, Peumans WJ. Characterisation and molecular cloning of two different type 2 ribosome-inactivating proteins from the monocotyledonous plant *Polygonatum multiflorum*. *Eur. J. Biochem.* 2000; **267**: 2746–2759.
19. Yeasmin T, Tang AK, Razzaque A, Absar N. Purification and characterization of three galactose specific lectins from mulberry seeds (*Morus* sp.). *Eur. J. Biochem.* 2001; **268**: 6005–6010.
20. Van Damme EJM, Roy S, Barre A, Citores L, Mostafapous K, Rouge P, Van Leuven F, Girbes T, Goldstein IJ, Peumans WJ. Elderberry (*Sambucus nigra*) bark contains two structurally different Neu5Ac(α2,6)Gal/GalNAc-binding type 2 ribosome-inactivating proteins. *Eur. J. Biochem.* 1997; **245**: 648–655.
21. Franz H, Ziska P, Kindt A. Isolation and properties of three lectins from mistletoe (*Viscum album* L.). *Biochem. J.* 1981; **195**: 481–484.
22. Eifler R, Pfüller K, Göckeritz W, Pfüller U. Improved procedures for isolation of mistletoe lectins and their subunits: lectin pattern of the european mistletoe. *Lectins: Biol. Biochem. Clin. Biochem.* 1993; **9**: 144–151.
23. Samtleben R, Kiefer M, Luther P. Characterization of the different lectins from *Viscum album* (Mistletoe) and their structural relationships with the agglutinins from *Abrus precatorius* and *Ricinus communis*. *Lectins: Biol. Biochem. Clin. Biochem.* 1985; **4**: 617–626.
24. Soler MH, Stoeva S, Schwarmborn C, Wilhelm S, Stiefel T, Voelter W. Complete amino acid sequence of the A chain of mistletoe lectin I. *FEBS Lett.* 1996; **399**: 153–157.
25. Soler MH, Stoeva S, Voelter W. Complete amino acid sequence of the B chain of mistletoe lectin I. *Biochem. Biophys. Res. Commun.* 1998; **246**: 596–601.
26. Ribereau-Gayon G, Jung ML, Frantz M, Anton R. Modulation of cytotoxicity and enhancement of cytokine release induced by *Viscum album* L. extracts or mistletoe lectins. *Anticancer Drugs* 1997; **8-1**: 3–8.
27. Joller PW, Menrad JM, Schwarz T, Pfüller U, Parnham MJ, Weyhenmeyer R, Lentzen H. Stimulation of cytokine production via a special standardized mistletoe preparation in an *in vitro* human skin bioassay. *Arzneimittelforsch./Drug Res.* 1996; **46**: 649–653.
28. Ribereau-Gayon G, Dumont S, Muller C, Jung ML, Poindron P, Anton R. Mistletoe lectins I, II and III induce the production of cytokines by cultured human monocytes. *Cancer Lett.* 1996; **109**: 33–38.
29. Büssing A, Suzart K, Schweizer K. Differences in the apoptosis-inducing properties of *Viscum album* L. extracts. *Anticancer Drugs* 1997; **8-1**: 9–14.
30. Büssing A, Suzart K, Bergmann J, Pfüller U, Schietzel M, Schweizer K. Induction of apoptosis in human lymphocytes treated with *Viscum album* L. is mediated by the mistletoe lectins. *Cancer Lett.* 1996; **99**: 59–72.
31. Altschul SF, Madden L, Schäffer AA, Zhang J, Zhang Z, Miller W, Lipman DJ. Gapped BLAST and PSI-BLAST: a new generation of protein database search programs. *Nucleic Acids Res.* 1997; **25**: 3389–3402.
32. Thompson JD, Gibson TJ, Plewniak F, Jeanmougin F, Higgins DG. The ClustalX windows interface: flexible strategies for multiple sequence alignment aided by quality analysis tools. *Nucleic Acids Res.* 1997; **25**: 4876–4882.
33. Nicholas KB, Nicholas HB Jr. GeneDoc: a tool for editing and annotating multiple sequence alignments. Distributed by the author 1997. URL: http://www.psc.edu/biomed/genedoc/.

34. Stoeva S, Maier T, Soler MH, Voelter W. Carbohydrate chains and their binding sites in mistletoe lectin I. *Polish J. Chem.* 1999; **73**: 125–133.
35. Debray H, Wieruszeski JM, Strecker G, Franz H. Structural analysis of the carbohydrate chains isolated from mistletoe (*Viscum album*) lectin I. *Carbohydr. Res.* 1992; **236**: 135–143.
36. Park CH, Lee DW, Kang TB, Lee KH, Yoon TJ, Kim JB, Do MS, Song SK. cDNA Cloning and sequence analysis of the lectin genes of the Korean mistletoe (*Viscum album coloratum*). *Mol. Cells* 2001; **12**: 215–220.
37. Yan X, Day P, Hollis T, Monzingo AF, Schelp E, Robertus JD, Milne GWA, Wang S. Recognition and interaction of small rings with the ricin A-chain binding site. *Proteins* 1998; **31**: 33–41.
38. Chen X, Link TM, Schramm VL. Ricin A-chain: Kinetics, mechanism, and RNA stem-loop inhibitors. *Biochemistry* 1998; **37**: 11 605–11 613.
39. Barbieri L, Battelli MG, Stirpe F. Ribosome-inactivating proteins from plants. *Biochim. Biophys. Acta* 1993; **1154**: 237–282.
40. Guex N, Peitsch MC. SWISS-MODEL and the Swiss-PdbViewer: An environment for comparative protein modelling. *Electrophoresis* 1997; **18**: 2714–2723.
41. Peitsch MC. ProMod and Swiss-Model: Internet-based tools for automated comparative protein modelling. *Biochem. Soc. Trans.* 1996; **24**: 274–279.
42. Peitsch MC. Protein modeling by e-mail. *Bio/Technology* 1995; **13**: 658–660.
43. URL: http://www.rcsb.org/pdb.
44. Eck J, Langer M, Möckel B, Rothe M, Zinke H, Lentzen H. Cloning of the mistletoe lectin gene and characterization of the recombinant A-chain. *Eur. J. Biochem.* 1999; **264**: 775–784.
45. Rutenber E, Katzin BJ, Ernst S, Collins EJ, Mlsna D, Ready MP, Robertus JD. Crystallographic refinement of ricin to 2.5 A. *Proteins* 1991; **10**: 240–250.
46. Henikoff S, Henikoff JG. Performance evaluation of amino acid substitution matrices. *Proteins* 1993; **17**: 49–61.
47. POV-Ray™ for Windows™, The Persistence of Vision Development Team, 1998.; URL: http://www.povray.org/.

